A Closed-Form CAD-Oriented Model for the High-Frequency Conductor Attenuation of Symmetrical Coupled Coplanar Waveguides

Giovanni Ghione, *Senior Member, IEEE*, and Michele Goano

***Abstract*— Closed-form CAD-oriented conformal-mapping approximations are presented for the HF attenuation of two-conductor symmetrical coupled coplanar waveguides (CCPW's). The expressions are compared with the results obtained from a full-wave electromagnetic (EM) simulator and found to yield acceptable agreement. A modified form is also presented according to [1], which partly overcomes the low-frequency limitations of the skin-effect approximation.**

***Index Terms*— Attenuation, conformal mapping, coplanar waveguides, couplers, design automation software, skin effect.**

I. Introduction

COUPLED coplanar waveguides (CCPW's) have application in several distributed components for hybrid and monolithic microwave integrated circuits (MMIC's) [2]. The cross section of the two-conductor symmetrical CCPW is shown in Fig. 1. Conformal-mapping expressions for the quasi-TEM parameters of CCPW's on infinite and finite-thickness substrates can be found in [2], [3]; however, to the authors' best knowledge, no closed-form model for the CCPW losses has been presented so far. In this paper a new closed-form expression for the HF (skin-effect) conductor attenuation of the CCPW is proposed. The exploited method is the conformal-mapping-analysis technique, formerly introduced by Owyang and Wu for the study of conductor losses in the symmetrical coplanar waveguide (CPW) with infinite lateral ground planes [4], and later extended by Ghione to general asymmetrical CPW's and striplines [5].

Although the well-known limitations of the skin-effect approach in the low-frequency range have been pointed out by several authors [6], [7], and shown to be significant in the modeling of integrated transmission lines, it can be suggested that closed-form expressions based on the skin-effect approach are still useful to the designer, since they yield the qualitatively correct behavior of the conductor attenuation versus the geometrical parameters of the line with relative errors, which are found in a typical coplanar example of the order of 12%–30% in comparison with more accurate numerical techniques [1, p. 2699]. In fact, such an error can be within the uncertainty often affecting the estimate of the metal conductivity.

Manuscript received October 8, 1996; revised March 24, 1997.

The authors are with the Dipartimento di Elettronica, Politecnico di Torino, I-10129, Torino, Italy.

Publisher Item Identifier S 0018-9480(97)04456-6.

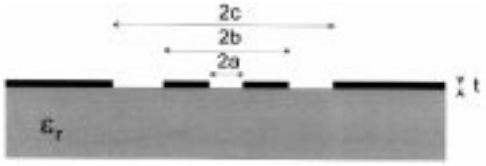

Fig. 1. Cross section of a two-conductor symmetrical CCPW on a semi-infinite dielectric substrate. The strip width is $w = b - a$, the central slot width is $s = 2a$, and the lateral slot width is $s_1 = c - b$.

Recently, an approach has been proposed by Holloway and Kuester [1] to account for both the low-frequency regime and the edge corrections at high frequency (i.e., when the strip thickness is much larger than the skin penetration depth). This method can be readily exploited to improve the overall accuracy of the present expressions.

The paper is structured as follows. Section II presents the relevant expressions for the HF attenuation of the even and odd modes, while in Section III modified expressions are developed to include the corrections in [1] and their predictions are validated against the results of an electromagnetic (EM) simulator [Hewlett-Packard's HF structure simulator (HFSS)]. Finally, some design remarks are presented regarding the behavior of the even- and odd-mode attenuations with respect to the centerband coupling and matching impedance of a two-conductor CCPW directional coupler. This behavior is found to be markedly different from the behavior of coupled microstrip lines.

II. Analysis

In this section, the ohmic loss analysis of a symmetrical CCPW according to the classical skin-effect HF approach is developed; moreover, the line thickness t is assumed to be suitably smaller than the line width $b-a$ and the slot widths $c-b$ and $2a$.

The per-unit-length conductor loss attenuation α_c^m of the odd ($m = o$) and even ($m = e$) mode of a two-conductor CPW may be expressed in terms of the modal resistance R^m as

$$\alpha_c^m = \frac{R^m}{2Z_c^m} \tag{1}$$

where Z_c^m is the characteristic impedance of the mode. The modal resistances are the eigenvalues of the resistance matrix $\mathbf{R}$ of the waveguide, which is symmetrical and reciprocal. In

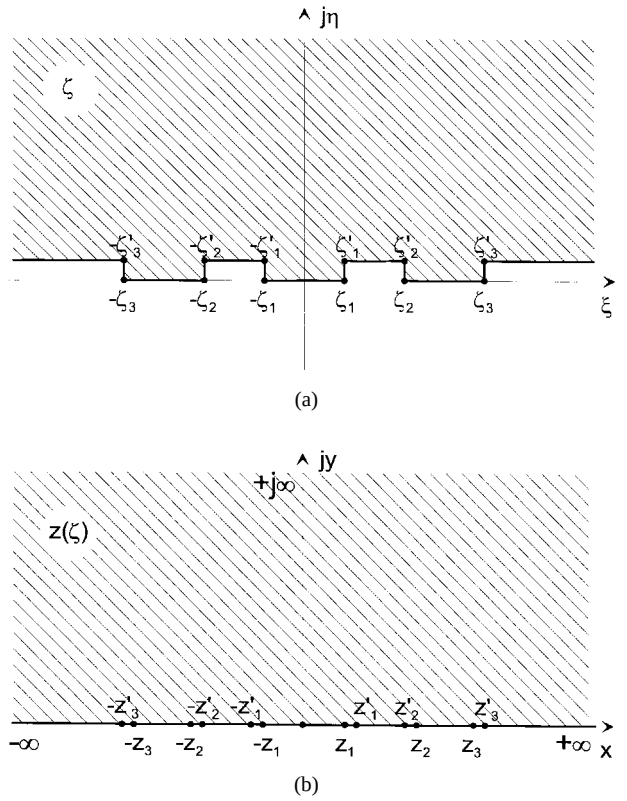

Fig. 2. (a) Mapping from the original ζ upper-half plane (thick lines) to (b) the upper-half z-plane (zero thickness lines).

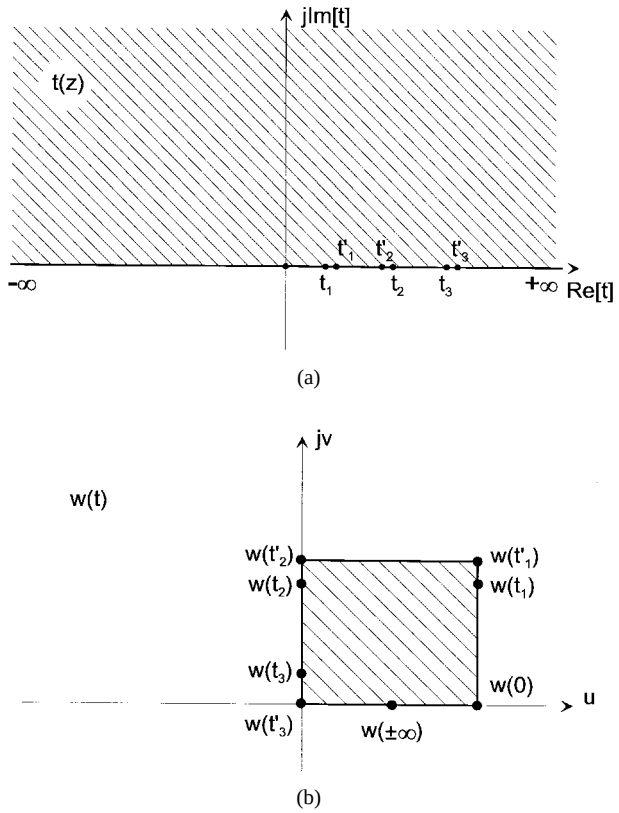

Fig. 3. Mapping from the $x > 0$, $y > 0$ quarter plane [see Fig. 2(b)] to (a) the upper half of the t plane and (b) final mapping to the interior of the rectangle in the w plane.

the case of a CCPW, $\mathbf{R}$ may be formally written as

$$\mathbf{R} = \begin{pmatrix} R & R_a \\ R_a & R \end{pmatrix}$$

whence

$$R^o = R - R_a$$
$$R^e = R + R_a.$$

Through the resistance matrix, the relationship between modal power dissipation and total current in each line $\mathbf{I} = (I_1\ I_2)$ is

$$P^m_{\text{diss}} = \mathbf{I} \cdot \mathbf{R} \cdot \mathbf{I}^T = RI_1^2 + RI_2^2 + 2R_aI_1I_2 = 2R^mI^2 \quad (2)$$

since $I_1 = -I_2 = I$ for the odd mode, $I_1 = I_2 = I$ for the even mode, and I is the total current carried by one line. Eventually by replacing (2) in (1), one recovers the well-known expression

$$\alpha_c^m = \frac{1}{2Z_c^m}\,\frac{P^m_{\text{diss}}}{2I^2} = \frac{R_s}{2Z_cI^2}\,\frac{1}{2}\oint |J_m|^2\,dl \quad (3)$$

where R_s is the surface resistance, J_m the modal current density, and the line integral is defined on the whole conductor periphery.

A. Odd Mode

Analytical approximations to the characteristic impedance of the odd mode of a CCPW have been presented in [2], [3]. In the case of thick substrate, both the odd- and the even-mode effective permittivity may be approximated as $\epsilon^o_{\text{eff}} = \epsilon^e_{\text{eff}} = \epsilon_{\text{eff}} = (1 + \epsilon_r)/2$, and one has

$$Z_c^o = \frac{60\pi}{\sqrt{\epsilon_{\text{eff}}}}\,\frac{K'(\beta_o)}{K(\beta_o)} \quad (4)$$

where

$$\beta_o = \sqrt{\frac{1 - k_{ab}^2}{1 - k_{ac}^2}}$$
$$k_{ab} = a/b$$
$$k_{bc} = b/c$$
$$k_{ac} = a/c$$

and K is the complete elliptic integral of the first kind.

Due to the symmetry of the structure, the integral of the current density has to be evaluated only on the upper half of the conductors (of thickness $t = 2\tau$) in the right half of plane ζ as follows:

$$\oint |J_o|^2\,dl = 2 \cdot 2 \cdot \left[\int_{\zeta_1}^{\zeta_2} |J_o(\zeta)|^2\,|d\zeta| + \int_{\zeta_3}^{\infty} |J_o(\zeta)|^2\,|d\zeta|\right] \quad (5)$$

where the factors 2 account for the symmetry along the x and y axis. The computation of these integrals is carried

out by applying the sequence of three conformal mappings represented in Figs. 2 and 3 as follows:

$$\left|\frac{dz}{d\zeta}\right| = \left|\sqrt{\frac{(z_1^2-z^2)(z_2^2-z^2)(z_3^2-z^2)}{(z_1'^2-z^2)(z_2'^2-z^2)(z_3'^2-z^2)}}\right| \tag{6}$$

$$\left|\frac{dt}{dz}\right| = |2z| \tag{7}$$

$$\left|\frac{dw}{dt}\right| = \left|\frac{1}{\sqrt{t(t-t_1)(t-t_2)(t-t_3)}}\right|. \tag{8}$$

The quarter plane $\Re\{\zeta\} > 0$, $\Im\{\zeta\} > 0$ is transformed in the interior of a rectangle in the w plane, and the current density is conveniently expressed in the intermediate z plane as

$$|J_o(z)| = \tilde{I}\left|\frac{dw}{dt}\right|\left|\frac{dt}{dz}\right|\left|\frac{dz}{d\zeta}\right| \tag{9}$$

where the scale factor $\tilde{I}$ represents the uniform current density in the w plane, and will not come into play in the final expression. Therefore, the integral (5) can be rewritten as

$$\begin{aligned}\int |J_o(\zeta)|^2\,|d\zeta| &= \int |J_o(z)|^2\,|dz| \\ &= 16\tilde{I}\left[\int_{z_1}^{z_2} P(z)\,|dz| + \int_{z_3}^{\infty} P(z)\,|dz|\right]\end{aligned} \tag{10}$$

where we have defined

$$\begin{aligned}P(z) = &\left|\frac{1}{\sqrt{(z_1^2-z^2)(z_2^2-z^2)(z_3^2-z^2)}}\right| \\ &\cdot\left|\frac{1}{\sqrt{(z_1'^2-z^2)(z_2'^2-z^2)(z_3'^2-z^2)}}\right|.\end{aligned}$$

The two integrals in (10) may be decomposed into eight different nonzero contributions [5, Appendix A], which can be approximated separately as

$$\begin{aligned}\int_{z_1}^{z_2} P(z)\,|dz| = &\int_{z_1}^{z_1'} P(z)\,|dz| + \int_{z_2'}^{z_2} P(z)\,|dz| \\ &+ \int_{z_1'}^{z_2'} Q_1(z)\,|dz| \\ &+ \int_{z_1'}^{z_1'+\epsilon} (P(z)-Q_1(z))\,|dz| \\ &+ \int_{z_2'-\epsilon}^{z_2'} (P(z)-Q_1(z))\,|dz|\end{aligned} \tag{11}$$

$$\begin{aligned}\int_{z_3}^{\infty} P(z)\,|dz| = &\int_{z_3}^{z_3'} P(z)\,|dz| + \int_{z_3'}^{\infty} Q_3(z)\,|dz| \\ &+ \int_{z_3'}^{z_3'+\epsilon} (P(z)-Q_3(z))\,|dz|\end{aligned} \tag{12}$$

where

$$\begin{aligned}Q_1(z) &= \frac{1}{(z^2-z_1^2)(z_2^2-z^2)(z_3^2-z^2)} \\ Q_3(z) &= \frac{1}{(z^2-z_1^2)(z^2-z_2^2)(z^2-z_3^2)}.\end{aligned}$$

Depending on the technique used for their approximation, two kinds of integrals can be distinguished. The first term in (11) is taken as a model of the first kind. By replacing $z_j' \approx z_j$ for $j \neq 1$ (i.e., far away from the singularity), and by developing $(z^2-z_1^2)(z_1'^2-z^2) = [(z+z_1)(z_1'+z)][(z-z_1)(z_1'-z)] \approx 4z_1^2(z-z_1)(z_1'-z)$, one has

$$\begin{aligned}&\int_{z_1}^{z_1'} P(z)\,|dz| \\ &\quad\approx \int_{z_1}^{z_1'} \frac{|dz|}{(z_2^2-z_1^2)(z_3^2-z_1^2)\sqrt{(z^2-z_1^2)(z_1'^2-z^2)}} \\ &\quad\approx \frac{1}{2z_1(z_2^2-z_1^2)(z_3^2-z_1^2)}\int_{z_1}^{z_1'} \frac{dz}{\sqrt{(z-z_1)(z_1'-z)}} \\ &\quad= \frac{\pi}{2}\frac{1}{z_1(z_2^2-z_1^2)(z_3^2-z_1^2)}.\end{aligned}$$

In the same way, one can evaluate

$$\begin{aligned}\int_{z_2'}^{z_2} P(z)\,|dz| &\approx \frac{\pi}{2}\frac{1}{z_2(z_2^2-z_1^2)(z_3^2-z_2^2)} \\ \int_{z_3}^{z_3'} P(z)\,|dz| &\approx \frac{\pi}{2}\frac{1}{z_3(z_3^2-z_1^2)(z_3^2-z_2^2)} \\ \int_{z_1'}^{z_1'+\epsilon} (P(z)-Q_1(z))\,|dz| &\approx \frac{\log 4}{2}\frac{1}{z_1(z_2^2-z_1^2)(z_3^2-z_1^2)} \\ \int_{z_2'-\epsilon}^{z_2'} (P(z)-Q_1(z))\,|dz| &\approx \frac{\log 4}{2}\frac{1}{z_2(z_2^2-z_1^2)(z_3^2-z_2^2)} \\ \int_{z_3'}^{z_3'+\epsilon} (P(z)-Q_3(z))\,|dz| &\approx \frac{\log 4}{2}\frac{1}{z_3(z_3^2-z_1^2)(z_3^2-z_2^2)}\end{aligned}$$

where the technique used to approximate the three integrals on a small interval of width ϵ in the neighborhood of the strip edges z_1', z_2', z_3' has been described in [5, eqs. (64)–(66)]. The second kind of integrals involves $Q_1(z)$ and $Q_3(z)$ alone, and requires partial fraction expansion. In the case of $Q_1(z)$, one has

$$\begin{aligned}Q_1(z) &= \frac{1}{(z-z_1)(z+z_1)(z_2-z)(z_2+z)(z_3-z)(z_3+z)} \\ &= \frac{1}{2z_1(z_2^2-z_1^2)(z_3^2-z_1^2)}\left(\frac{1}{z-z_1}-\frac{1}{z+z_1}\right) \\ &\quad+\frac{1}{2z_2(z_2^2-z_1^2)(z_3^2-z_2^2)}\left(\frac{1}{z_2-z}-\frac{1}{z_2+z}\right) \\ &\quad-\frac{1}{2z_3(z_3^2-z_1^2)(z_3^2-z_2^2)}\left(\frac{1}{z_3-z}-\frac{1}{z_3+z}\right).\end{aligned}$$

Since the strip thickness is much smaller than the distance between the strip edges, one can approximate (see the discussion in [5, p. 1502])

$$z_i' - z_j \approx \begin{cases} z_i - z_j, & \text{if } i \neq j \\ 2\tau/\pi, & \text{if } i = j \end{cases}$$

and the integral becomes

$$\begin{aligned}\int_{z_1'}^{z_2'} & Q_1(z)\,|dz| \\ &= \frac{1}{2z_1(z_2^2-z_1^2)(z_3^2-z_1^2)}\log\left(\frac{\pi}{\tau}z_1\frac{z_2-z_1}{z_2+z_1}\right) \\ &\quad + \frac{1}{2z_2(z_2^2-z_1^2)(z_3^2-z_2^2)}\log\left(\frac{\pi}{\tau}z_2\frac{z_2-z_1}{z_2+z_1}\right) \\ &\quad + \frac{1}{2z_3(z_3^2-z_1^2)(z_3^2-z_2^2)}\log\left(\frac{\pi}{\tau}\frac{z_3-z_2}{z_3+z_2}\frac{z_3+z_1}{z_3-z_1}\right).\end{aligned}$$

In the same way, one can evaluate

$$\begin{aligned}\int_{z_3'}^{\infty} & Q_3(z)\,|dz| \\ &\approx \frac{1}{2z_1(z_2^2-z_1^2)(z_3^2-z_1^2)}\log\left(\frac{z_3+z_1}{z_3-z_1}\right) \\ &\quad + \frac{1}{2z_2(z_2^2-z_1^2)(z_3^2-z_2^2)}\log\left(\frac{z_3-z_2}{z_3+z_2}\right) \\ &\quad + \frac{1}{2z_3(z_3^2-z_1^2)(z_3^2-z_2^2)}\log\left(\frac{\pi}{\tau}z_3\right).\end{aligned}$$

On the whole, integral (5) may be expressed as

$$\begin{aligned}\oint |J_o|^2\,dl = 8\tilde{I}\Bigg\{ & \frac{1}{z_1(z_2^2-z_1^2)(z_3^2-z_1^2)} \\ & \cdot\left[\log\left(\frac{8\pi}{t}z_1\frac{z_2-z_1}{z_2+z_1}\frac{z_3+z_1}{z_3-z_1}\right)+\pi\right] \\ & + \frac{1}{z_2(z_2^2-z_1^2)(z_3^2-z_2^2)} \\ & \cdot\left[\log\left(\frac{8\pi}{t}z_2\frac{z_2-z_1}{z_2+z_1}\frac{z_3-z_2}{z_3+z_2}\right)+\pi\right] \\ & + \frac{1}{z_3(z_3^2-z_1^2)(z_3^2-z_2^2)} \\ & \cdot\left[\log\left(\frac{8\pi}{t}z_3\frac{z_3+z_1}{z_3-z_1}\frac{z_3-z_2}{z_3+z_2}\right)+\pi\right]\Bigg\}.\end{aligned} \tag{13}$$

Neglecting the conductor thickness, the total current I_{odd} carried by one strip can be evaluated as

$$\begin{aligned}I_o &= 2\cdot\int_{z_1}^{z_2}\frac{2\tilde{I}\,dz}{\sqrt{(z^2-z_1^2)(z_2^2-z^2)(z_3^2-z^2)}} \\ &= \frac{4\tilde{I}K(\beta_o)}{z_2\sqrt{z_3^2-z_1^2}}.\end{aligned} \tag{14}$$

Eventually, by approximating $z_i - z_j \approx \zeta_i - \zeta_j$ and by replacing (4), (13), and (14) in (3), the ohmic attenuation of the odd mode may be expressed as

$$\begin{aligned}\alpha_c^o = \frac{R_s\sqrt{\epsilon_{\text{eff}}}(1-k_{ac}^2)}{480\pi K(\beta_o)K(\beta_o')}\Bigg\{ & \frac{1}{a}\frac{1}{(1-k_{ab}^2)(1-k_{ac}^2)} \\ & \cdot\left[\log\left(\frac{8\pi a}{t}\frac{1-k_{ab}}{1+k_{ab}}\frac{1+k_{ac}}{1-k_{ac}}\right)+\pi\right] \\ & + \frac{1}{b}\frac{1}{(1-k_{ab}^2)(1-k_{bc}^2)} \\ & \cdot\left[\log\left(\frac{8\pi b}{t}\frac{1-k_{ab}}{1+k_{ab}}\frac{1-k_{bc}}{1+k_{bc}}\right)+\pi\right] \\ & + \frac{1}{c}\frac{k_{bc}^2}{(1-k_{ac}^2)(1-k_{bc}^2)} \\ & \cdot\left[\log\left(\frac{8\pi c}{t}\frac{1+k_{ac}}{1-k_{ac}}\frac{1-k_{bc}}{1+k_{bc}}\right)+\pi\right]\Bigg\}.\end{aligned} \tag{15}$$

B. Even Mode

The characteristic impedance of the even mode is [2], [3]

$$Z_c^e = \frac{60\pi}{\sqrt{\epsilon_{\text{eff}}}}\frac{K'(\beta_{\text{e}})}{K(\beta_{\text{e}})} \tag{16}$$

where

$$\beta_{\text{e}} = k_{bc}\sqrt{\frac{1-k_{ab}^2}{1-k_{ac}^2}}.$$

The expression for the ohmic losses of the even mode may be found by following the same derivation presented for the odd mode. The only difference is that the conformal mapping (8) has to be replaced by

$$\left|\frac{dw}{dt}\right| = \left|\frac{1}{\sqrt{(t-t_1)(t-t_2)(t-t_3)}}\right| \tag{17}$$

where the singularity in the origin has been removed because the symmetry axis y is now behaving as a magnetic plane. Hence, the current density integral becomes

$$\int |J_{\text{e}}(\zeta)|^2\,|d\zeta| = 16\tilde{I}\left[\int_{z_1}^{z_2}P(z)|z|^2\,|dz| + \int_{z_3}^{\infty}P(z)|z|^2\,|dz|\right]$$

while the total current I_e carried by one line may be approximated as

$$\begin{aligned}I_e &= 2\int_{z_1}^{z_2}\frac{2\tilde{I}z\,dz}{\sqrt{(z^2-z_1^2)(z_2^2-z^2)(z_3^2-z^2)}} \\ &= \frac{4\tilde{I}K(\beta_e)}{\sqrt{z_3^2-z_1^2}}\end{aligned}$$

and one eventually obtains

$$\begin{aligned}\alpha_c^e = \frac{R_s\sqrt{\epsilon_{\text{eff}}}(1-k_{ac}^2)}{480\pi K(\beta_e)K(\beta_e')}\Bigg\{ & \frac{1}{a}\frac{k_{ab}^2}{(1-k_{ab}^2)(1-k_{ac}^2)} \\ & \cdot\left[\log\left(\frac{8\pi a}{t}\frac{1-k_{ab}}{1+k_{ab}}\frac{1+k_{ac}}{1-k_{ac}}\right)+\pi\right] \\ & + \frac{1}{b}\frac{1}{(1-k_{ab}^2)(1-k_{bc}^2)}\end{aligned}$$

$$\cdot \left[\log\left(\frac{8\pi b}{t}\frac{1-k_{ab}}{1+k_{ab}}\frac{1-k_{bc}}{1+k_{bc}}\right)+\pi\right] + \frac{1}{c}\frac{1}{(1-k_{ac}^2)(1-k_{bc}^2)} \cdot \left[\log\left(\frac{8\pi c}{t}\frac{1+k_{ac}}{1-k_{ac}}\frac{1-k_{bc}}{1+k_{bc}}\right)+\pi\right]\right\}. \quad (18)$$

III. Results and Discussion

In order to validate the above expressions for the even- and odd-mode attenuations, several CCPW's on a thick GaAs substrate ($\epsilon_r = 12.9$) were simulated by means of the Hewlett-Packard HFSS EM simulator.[1] Even and odd excitation was accomplished by simulating only half of the structure, with ideal E-type or H-type boundary conditions on the symmetry plane. The ports-only solution mode (see footnote 1, p. A13) was exploited, whereby the simulator solves a two-dimensional (2-D) eigenvalue problem on the waveguide cross section. Since the skin-effect approach is only valid at high frequency (i.e., for strip thickness suitably larger than the skin penetration thickness) the simulations were performed with HFSS by imposing surface-impedance boundary conditions on the line conductors.

Although the present analytical approach is based on a surface-resistance formulation implying, for smooth surfaces, surface-impedance boundary conditions, some problems may arise near conductor edges, as suggested in [1]. For the sake of comparison, the modified approach of [1] was also implemented. For the coupled line case, the equivalent of [1, eq. (15)] reads

$$\alpha_c^m \approx \Re\left(\frac{2A^m}{1+\sqrt{1+4A^m/\gamma^m}}\right) \quad (19)$$

where $\gamma^m = jk_0\sqrt{\epsilon_{\text{eff}}^m}$, and k_0 is the free-space wavenumber. The parameters A^m may be obtained from the expressions of the ohmic losses (15) and (18) derived in Section II, by replacing the surface resistance R_s with $Z_s + Z_m$, and the terms $\frac{8\pi}{t}$ in the arguments of the logarithms with $\frac{2}{\Delta}$. The surface impedances Z_s and Z_m are defined in [1, p. 2696], while Δ is the modified stopping distance given in [1, Table I]. The interest in the modified approach also lies in the fact that it partly overcomes the low-frequency limitations of the skin-effect formulation, while preserving completely analytical expressions, since the stopping distance Δ can be easily recovered by spline approximation of the data in [1, Table I].

An example of the results obtained is shown in Fig. 4. The overall behavior of the attenuation as evaluated with HFSS is in qualitative agreement with the present approach (continuous line) but the values obtained typically are 10%–20% larger than the HFSS values. The results obtained from the modified formulas (19) are shown in Fig. 4, dashed line; although the agreement with the numerical simulation is slightly better, the discrepancy is still fairly high in the absolute values. The same trend is also found in other computations not shown here for the sake of brevity. A similar behavior of HFSS was also detected by other authors [8]. Convergence studies carried out on the HFSS simulator reveal that a slight increase in the attenuation can be detected by improving the simulation accuracy (in the results shown, a 0.01% port field accuracy was used). Unfortunately, the convergence study cannot be pushed beyond a certain limit because of the ensuing computational intensity. It may also be argued that owing to the presence of square-integratable singularities in the solution, the polynomial FEM approximation exploited by HFSS exhibits very slow convergence *versus* the discretization density.

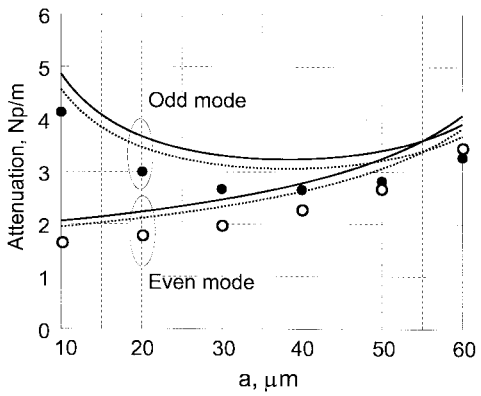

Fig. 4. Even and odd-mode attenuations for a CCPW on a thick GaAs substrate as a function of the slot half-width a. The frequency is 5 GHz, the strip width w is 70 μm, the strip thickness t is 5 μm, and the half-spacing between the ground planes is 150 μm. For the strip conductivity $\sigma = 5.8\times10^7$ S/m was assumed. The continuous line is the present approach; the dashed line is the same, with the edge corrections in [1]; the circles are results from the HFSS simulator.

To investigate the behavior of the CCPW losses with respect to the typical design parameters of a coplanar directional coupler, the even- and odd-mode attenuation of a CCPW on a thick GaAs substrate as a function of the coupler centerband coupling C and matching impedance Z_0 were evaluated. The ground plane spacing $2c = 300$ μm refers to a monolithic implementation, and the line thickness is $t = 2.5$ μm. The results are shown in Fig. 5 as a function of the centerband coupling, taking as a parameter the matching impedance. The upper and lower coupling corresponds for each curve to line-to-ground or line-to-line spacing being twice as the line thickness, i.e., 5 μm. Besides being a reasonable technological limit, tighter spacing would require substantial corrections in the odd mode effective permittivity [9, Sec. 7.3.1] with respect to the ideal (zero-thickness) line value used here. The behavior of the even- and odd-mode losses is fairly similar for low C; in particular, the attenuation of both modes increases with decreasing coupling and decreasing matching impedance. This behavior can be explained by taking into account that low coupling between conductors implies low spacing between each conductor and the lateral ground plane, thereby increasing edge effects and losses. This phenomenon is even more pronounced with low Z_0, since in this case the strip width is larger, thus leading to an even greater coupling to the lateral ground planes. The increase of losses with decreasing Z_0 and C is in contrast with the behavior of microstrip couplers, whose losses typically decrease with decreasing coupling and matching impedance. For high C (e.g., larger than -10 dB) the

[1] Hewlett-Packard Company, Santa Rosa, CA, *HP 85180A High-Frequency Structure Simulator, User's Reference*, May 1992.

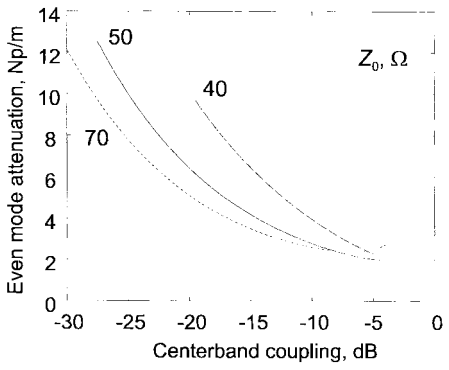

(a)

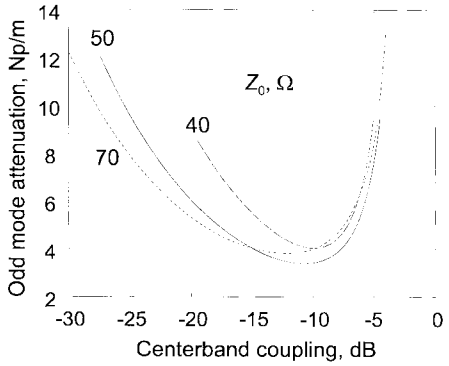

(b)

Fig. 5. (a) Even- and (b) odd-mode attenuations for a coplanar coupler on thick GaAs substrate ($f = 5$ GHz, $t = 2.5$ μm, $c = 150$ μm) as a function of the centerband coupling, having as a parameter the matching impedance. For the strip conductivity $\sigma = 5.8 \times 10^7$ S/m was assumed.

odd-mode losses increase owing to the tight coupling between strip edges (as in coupled microstrips), whereas the even-mode attenuation is almost constant.

To summarize, the analysis shows that low losses are not obtained with low couplings (as in microstrip couplers) but rather with intermediate values (for instance, around −10 dB). Tight couplings lead to an overall increase of losses apart from feasibility considerations related to technological limitations on the central slot width.

IV. Conclusion

Closed-form CAD-oriented conformal-mapping approximations for the HF attenuation of symmetrical two-conductor CCPW's have been developed. The expressions are in fairly good agreement with the results obtained from a full-wave EM simulator. Some design considerations are developed on the behavior of losses as a function of the coupling and matching impedance of a two-conductor CCPW coupler.

Acknowledgment

The authors wish to thank an anonymous reviewer for his comments and useful suggestions.

References

[1] C. L. Holloway and E. F. Kuester, "A quasi-closed-form expression for the conductor loss of CPW lines, with an investigation of edge shape effects," *IEEE Trans. Microwave Theory Tech.*, vol. 43, pp. 2695–2701, Dec. 1995.
[2] C. P. Wen, "Coplanar-waveguide directional couplers," *IEEE Trans. Microwave Theory Tech.*, vol. MTT-18, pp. 318–322, June 1970.
[3] V. F. Hanna and D. Thebault, "Analyze des couplers directifs coplanaires," *Ann. Télécommun.*, vol. 39, nos. 7–8, pp. 299–306, 1984.
[4] G. H. Owyang and T. T. Wu, "The approximate parameters of slot lines and their complement," *IRE Trans. Antennas Propagat.*, vol. AP-6, pp. 49–55, Jan. 1958.
[5] G. Ghione, "A CAD-oriented analytical model for the losses of general asymmetric coplanar lines in hybrid and monolithic MIC's," *IEEE Trans. Microwave Theory Tech.*, vol. 41, pp. 1499–1510, Sept. 1993.
[6] W. Heinrich, "Full-wave analysis of conductor losses on MIMIC transmission lines," *IEEE Trans. Microwave Theory Tech.*, vol. 38, pp. 1468–1472, Oct. 1990.
[7] E. Tuncer, B.-T. Lee, M. S. Islam, and D. P. Neikirk, "Quasi-static conductor loss calculations in transmission lines using a new conformal mapping technique," *IEEE Trans. Microwave Theory Tech.*, vol. 42, pp. 1807–1815, Sept. 1994.
[8] G. G. Gentili and A. Melloni, "The incremental inductance rule in quasi-TEM coupled transmission lines," *IEEE Trans. Microwave Theory Tech.*, vol. 43, pp. 1276–1280, June 1995.
[9] K. C. Gupta, R. Garg, and I. J. Bahl, *Microstrip Lines and Slotlines*. Norwood, MA: Artech House, 1979.
[10] K.-K. M. Cheng, "Analysis and synthesis of coplanar coupled lines on substrates of finite thicknesses," *IEEE Trans. Microwave Theory Tech.*, vol. 44, pp. 636–639, Apr. 1996.
[11] M. R. Lyons and C. A. Balanis, "Transient coupling reduction and design considerations in edge-coupled coplanar waveguide couplers," *IEEE Trans. Microwave Theory Tech.*, vol. 44, pp. 778–783, May 1996.

Giovanni Ghione (M'87–SM'94) was born in Alessandria, Italy, in 1956. He graduated *cum laude* from Politecnico di Torino, Torino, Italy, in 1981.

In 1983, he was a Research Assistant with Politecnico di Torino. From 1987 to 1990, he was an Associate Professor with Politecnico di Milano, Milan, Italy. In 1990, he joined the University of Catania, Catania, Italy, as a Full Professor of electronics. Since 1991, he has been a Full Professor of electronics at Politecnico di Torino, as part of the II faculty of engineering. He has published over 100 papers and book chapters. Since 1981, he has been engaged in Italian and European research projects (ESPRIT 255, COSMIC, and MANPOWER) in the field of active and passive microwave CAD. His present research interests concern the physics-based simulation of active microwave and optoelectronic devices, with particular attention to noise modeling, thermal modeling, and active device optimization. His research interests also include several topics in computational electromagnetics, including coplanar component analysis.

Mr. Ghione is a member of the Editorial Board for IEEE Transactions on Microwave Theory and Techniques and a member of the Associazione Elettrotecnica Italiana (AEI).

Michele Goano was born in 1965 in Torino, Italy. He received the Laurea and the Ph.D. degrees in electronic engineering from Politecnico di Torino, Torino, Italy, in 1989 and 1993, respectively.

From 1994 to 1995, he was a Post-Doctoral Fellow in the Département de Génie Physique of École Polytechnique de Montréal, Montreal, P.Q., Canada. Since 1996, he has been a Research Assistant at the Dipartimento di Elettronica, Politecnico di Torino. He has been engaged in modeling of semiconductor optical components and Monte Carlo simulation of quantum-well devices. He is currently involved in research on coplanar components and traveling-wave photodetectors.